Laboratory Investigation (2021) 101:1026–1035
https://doi.org/10.1038/s41374-021-00596-4

ARTICLE

# MiR-181b suppresses angiogenesis by directly targeting cellular communication network factor 1

Yue Li[1,2] · Siyuan Fan[1,2] · Weichang Xia[3] · Baoru Qiao[4] · Kai Huang[1,2] · Jingqun Zhou[3] · Minglu Liang[1]

Received: 5 October 2020 / Revised: 24 March 2021 / Accepted: 25 March 2021 / Published online: 19 April 2021


## Abstract

Angiogenesis is essential for various physiological and pathological processes. Previous studies have shown that miRNAs play an important role in blood vessel development and angiogenesis. Recent studies have suggested that miR-181b might be involved in the regulation of angiogenesis in tumors. However, whether miR-181b plays a role in angiogenesis in nontumor diseases is unclear. We found that miR-181b expression was downregulated in hypoxia-stimulated primary human umbilical vein endothelial cells (HUVECs) and a mouse hindlimb ischemia (HLI) model. Gain- and loss-of-function studies showed that a miR-181b mimic inhibited HUVEC migration and tube formation in vitro, and a miR-181b inhibitor had the opposite effects. In vivo, agomir-181b suppressed perfusion recovery in the HLI model and capillary density in a Matrigel plug assay, while perfusion recovery and capillary density were increased by injection of antagomir-181b. Mechanistically, we showed with a reporter assay that cellular communication network factor 1 (CCN1) was a direct target of miR-181b. Moreover, miR-181b suppressed angiogenesis at least in part by targeting CCN1 to inhibit the AMPK signaling pathway. Our research suggests that miR-181b suppresses angiogenesis by directly targeting CCN1, which provides new clues for pro-angiogenic treatment strategies.

## Introduction

Peripheral arterial disease (PAD) is caused by peripheral arterial stenosis. When large blood vessels are blocked, patients with PAD require therapies to promote the growth of new blood vessels (therapeutic angiogenesis). The prognosis of PAD patients is closely related to the degree of angiogenesis in ischemic tissues, which can reconstitute the supply of oxygen and nutrients and is beneficial for tissue repair and functional recovery. Therefore, exploring the mechanism of angiogenesis is of great significance for elucidating the pathogenesis of related diseases and developing effective prevention and treatment strategies [1–4].

Angiogenesis mainly refers to the process by which microvessels sprout from the existing vascular bed and form new blood vessel branches and capillary plexus. Although most of the body's blood vessels remain stationary in adulthood, vascular endothelial cells can still rapidly divide in response to pathological stimulation, causing activation of angiogenesis [5, 6]. Various factors, including vascular endothelial growth factor (VEGF), basic fibroblast growth factor (bFGF), angiogenin (Ang), transforming growth factor, platelet-derived growth factor, and endothelial growth factor (EGF), act on vascular cells through different

These authors contributed equally: Yue Li, Siyuan Fan

**Supplementary information** The online version contains supplementary material available at https://doi.org/10.1038/s41374-021-00596-4.

✉ Kai Huang
Huangkai1@hust.edu.cn

✉ Jingqun Zhou
Jingqunzhou@163.com

✉ Minglu Liang
liangml@hust.edu.cn

[1] Clinic Center of Human Gene Research, Union Hospital, Tongji Medical College, Huazhong University of Science and Technology, Wuhan, China

[2] Department of Cardiology, Union Hospital, Tongji Medical College, Huazhong University of Science and Technology, Wuhan, China

[3] Affiliated Renhe Hospital to China Three Gorges University, Yichang City, China

[4] Department of Vascular Surgery, Union Hospital, Tongji Medical College, Huazhong University of Science and Technology, Wuhan, China

pathways and interact and cooperate with each other to promote angiogenesis; the VEGF family members are the most important factors in the process of angiogenesis [7]. Hypoxia promotes high levels of VEGF expression and forms a VEGF concentration gradient in hypoxic tissues. VEGF binds to its receptor on endothelial cells to activate downstream signaling cascades. In response to VEGF stimulation, vascular endothelial cells are rapidly activated to migrate to a distance and form new primary capillaries based on the existing vascular network [8, 9].

MicroRNAs are single-stranded noncoding RNAs with lengths of ~22 nucleotides. MicroRNAs regulate gene expression by inhibiting the translation or promoting the degradation of target mRNAs. The multidomain protein dicer is responsible for processing miRNA precursor molecules into mature miRNAs. Dicer homozygous mutant mice die during the period from E12.5 to 14.5 during embryonic development, and microscopy experiments have revealed that the yolk sac of homozygous mutant mice have significantly fewer blood vessels than the yolk sac of normal mice, indicating that miRNAs play an essential role in the process of embryonic blood vessel formation [10]. MiRNAs also play essential roles in the compensatory mechanisms of vascular occlusive diseases. Bonauer et al. found that after femoral artery ligation, treating mice with antagomir, which specifically inhibits miR-92a, promotes hemoperfusion recovery in hind limbs [11]. Subsequently, Grundmann et al. found that the use of antagomirs to inhibit miR-100 can also facilitate the recovery of limb blood supply in mice [12]. Our research aims to reveal the role of miR-181b in angiogenesis in ischemic diseases and the underlying mechanism.

## Materials and methods

### Reagents and antibodies

The antibodies against cellular communication network factor 1 (CCN1) (14,479, 1:1000), AMPK (5832, 1:1000), p-AMPK (50,081, 1:1000), and GAPDH (5174, 1:1000) were purchased from Cell Signaling Technology (USA). The antibodies against α-SMA (ab5694, 1:200) were purchased from Abcam (USA). Isolectin (IB4, L2895) was purchased from Sigma (USA). The HRP-conjugated Affinipure Goat Anti-Mouse IgG (H + L) (SA00001-1, 1:3000) and HRP-conjugated Affinipure Goat Anti-Rabbit IgG (H + L) (SA00001-2, 1:3000) were purchased from Proteintech (China). The anti-rabbit IgG (H + L), F(ab′)2 Fragment (Alexa Fluor® 594 Conjugate) (8889S, 1:500), anti-rabbit IgG (H + L), F(ab′)2 Fragment (Alexa Fluor® 594 Conjugate) (4408S, 1:500) were purchased from Cell Signaling Technology.

### Cell culture

For cell culture, primary human umbilical vein endothelial cells (HUVECs) were maintained in ECM and cultured according to the instructions provided by the supplier. HUVECs in passages between 3 and 7 were used in all the experiments. 293T cells were cultured in DMEM with 10% FBS and 1% penicillin/streptomycin solution at 37 °C and in 5% $CO_2$. For the hypoxia experiment, HUVECs were treated under the conditions of 1% $O_2$, 5% $CO_2$, and 94% $N_2$ for 24 h. For adenovirus infection, ad-GFP, ad-CCN1, ad-scramble sh, and ad-CCN1 sh were purchased from OBiO technology (Shanghai, China) and infected following the instructions. All procedures performed in studies involving human participants were conducted in accordance with the 1964 Declaration of Helsinki and its later amendments or comparable ethical standards. Informed consent was obtained from all the individual participants included in the study.

### Mice

Male wild-type (WT, C57BL/6 background) mice aged 8 weeks and weighing 25–29 g were purchased from Tongji Medical College of Huazhong University of Science and Technology. All the experimental designs were approved by the Ethics Committee of Tongji Medical College of Huazhong University of Science and Technology and conducted in compliance with the guidelines and regulations of the state and relevant institutions.

### Mouse model of hindlimb ischemia

Eight-week-old male C57BL/6 mice were used to establish the hindlimb ischemia (HLI) model. For the gain- and loss-of-function experiments, C57BL/6 mice were intramuscularly injected with either agomir-negative control (agomir-NC), agomir-181b, antagomir-negative control (antagomir-NC), or antagomir-181b (5 nM). The injections were administered at three sites in the gastrocnemius muscle on days 0, 4, and 10 after HLI was induced. The mice were anesthetized with sodium pentobarbital (60 mg/kg body weight) by intraperitoneal injection, and the surgical operations were performed under sterile conditions. The mice were placed in the preoperating area on a warming pad at 37 °C. Then, the hair on the right hindlimbs was shaved. The right superficial and deep femoral arteries were bluntly ligated and excised to induce HLI, and the skin was overly closed. All the veins and nerves were carefully cared for and were not damaged during the operation. Several days after the operation, the gastrocnemius muscles were excised, embedded in paraffin or stored at −80 °C and were later prepared for immunostaining and RT-qPCR analysis, respectively.

## Laser Doppler perfusion images

The blood flow of the ischemic (right) limb and normal (left) limb was measured using laser Doppler perfusion imaging (Perimed) on postoperative days 0, 1, 2, 3, 4, 7, and 14. First, the mice were placed in a supine position on a warming pad at 37 °C. Then, the region of interest was focused on by consecutively measuring the intensity of the blood flow. Color-coded images were recorded, and analyses were automatically performed by calculating the average perfusion of each limb. The perfusion ratio calculated from the blood flow of the right (contracted) and left (normal) legs of each animal was used to assess limb circulation.

## Quantitative RT-PCR

Total RNA was isolated from HUVECs and muscle tissues of the mice using TRIzol (Takara) and standard methods. The isolated RNA was then reverse transcribed into cDNA using the RR037A PrimeScript™ RT reagent Kit (Perfect Real Time; Takara). To detect the levels of microRNAs (miRs), stem-loop quantitative reverse transcription-PCR (RT-PCR) was used. The stem-loop primer was purchased from RiboBio (Guangzhou, China). Then, qRT-PCR was performed using SYBR Green master mix (Vazyme, Nanjing, China). Each sample was analyzed in duplicate, and the miRNA expression was normalized to that of its respective U6 mRNA. Other genes were analyzed using GAPDH mRNA expression as the internal control. All the fold changes in gene expression were analyzed by the $2^{-\Delta\Delta CT}$ method.

## Transwell migration assay

HUVECs were first transfected with miR-181b mimic, inhibitor or negative control (NC) RNAs in a six-well plate. Then, $4 \times 10^4$ HUVECs were detached and suspended in 200 µl ECM, mixed with human VEGF (10 ng/ml, Peprotech), and placed into the upper chamber (8.0 µm pore size, Corning), which was coated with 15 µg/ml rat tail collagen. Next, the chamber was placed in a 24-well plated and cultured in complete medium. After incubation for 4 h at 37 °C, the migrated cells were fixed with 4% paraformaldehyde for 15 min and stained with 0.1% crystal violet for 15 min. Finally, six randomly chosen fields were photographed by microscopy (Olympus).

## Tube formation assay

For the tube formation assay, each well of 96-well plates was first precoated with 50 µl of Matrigel (356234, Corning). Next, HUVECs were transfected with miR-181b mimic, inhibitor or NC RNAs in a six-well plate for 24 h. Then, these HUVECs were detached from the six-well plate, mixed with human VEGF (10 ng/ml, Peprotech) and suspended into each well of the Matrigel-precoated 96-well plate at a density of $1 \times 10^4$ cells/well. The plates were then incubated at 37 °C in 5% $CO_2$ for 4 h. Tube formation was observed under a microscope (Olympus).

## Matrigel plug assay

Then, 500 µl Matrigel containing cells that were pre-transfected with agomir-181b, antagomir-181b, or scramble, heparin (60 U, Sigma-Aldrich) and bFGF (150 ng/ml, Peprotech) were subcutaneously injected into 6–8-week-old female athymic nude mice (Charles River, China) along the abdominal midline. Seven days later, the mice were euthanized, and the implants were harvested. Then, Matrigel plugs were embedded in paraffin for hematoxylin and eosin (H&E) staining.

## Immunofluorescence

Fourteen days after HLI surgery, the paraffin-embedded ischemic gastrocnemius muscles were sectioned in increments of 4 µm, immunostained with IB4 and α-SMA antibodies (ab5694; Abcam), and then incubated with the indicated secondary antibodies. The new capillary density was analyzed by randomly counting 10 fields of view (magnification ×100) and are expressed as IB4+ and α-SMA+ areas.

## Plasmid constructs and luciferase reporter assay

The negative control mimic (NC mimic) and miR-181b mimic (RboBio, China) were transfected with Lipofectamine 2000 (Invitrogen) following the manufacturer's manuals. We used TargetScan (http://www.targetscan.org) to predict the target genes and binding sites. In terms of the luciferase reporter assay, the fragments of the CCN1 3′UTR containing the miR-181b binding sequence or the mutated sequence were ligated into the psiCHECK dual-luciferase vector (Promega). Then, the dual-luciferase reporter vector was transiently transfected into HEK293T cells along with the miR-181b mimic or NC mimic. The luciferase activity was measured by the Dual-Luciferase Reporter Gene Assay Kit (Beyotime, RG027) following the manufacturer's manual.

## Western blot analysis

The HUVECs were lysed, and the total protein was extracted using RIPA lysis buffer with 1 mM PMSF. Then, the proteins (20 µg) were separated by 10% SDS-polyacrylamide gel electrophoresis and electrotransferred onto polyvinylidene difluoride (PVDF) membranes (Millipore). After washing with TBS-T, the membranes were incubated with primary antibodies overnight at 4 °C and with horseradish

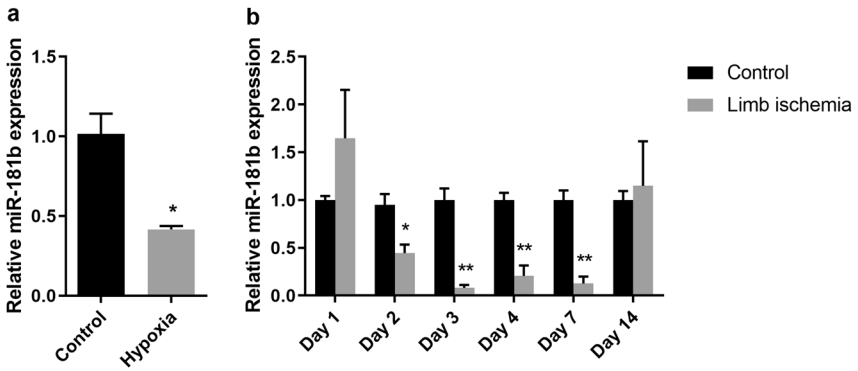


**Fig. 1 miR-181b was altered in cellular stimulation and animal models. a** miR-181b was downregulated in HUVECs after exposure to hypoxia for 24 h. Data are presented as the mean ± SEM ($n = 3$), $^*p < 0.05$ compared with control (normoxia). **b** Expression of miR-181b was detected in ischemic muscle tissue compared with nonischemic control muscle tissue on various days after ischemia. Data are presented as the mean ± SEM ($n = 3$), $^*p < 0.05$; $^{**}p < 0.01$ compared with the control (nonischemia).

peroxidase-conjugated secondary antibodies for 1 h at room temperature. Immunoreactive signals were detected by ChemiDoc Imaging Systems (Bio-Rad).

### Human tissue studies

Expressional studies were performed on muscular specimens taken from either amputated legs of diabetic patients ($n = 3$) or in nondiabetic patients with a car accident (controls, $n = 3$). Studies complied with the ethical principles stated in the Declaration of Helsinki and were approved by the Ethics Committee of Tongji Medical College of Huazhong University of Science and Technology. Patients gave written informed consent to sample collection.

### Statistical analysis

GraphPad Prism software (GraphPad Software, Inc., San Diego, CA) was used for the statistical analyses. Comparisons between two groups were made by Student's $t$ test. $P$ values < 0.05 were considered to be significant.

## Results

### miR-181b was downregulated in HUVECs subjected to hypoxia and hindlimb muscle tissues subjected to ischemia

Previous studies have shown that miR-181b plays a critical role in tumor-associated angiogenesis. However, miR-181b-regulated biological behaviors and angiogenesis of HUVECs in nontumor models have not been well studied. Therefore, we tested the miR-181b levels in hypoxia-treated HUVECs and found that miR-181b expression was downregulated compared with its expression in normoxia-treated HUVECs (Fig. 1a).

To further understand the function of miR-181b in angiogenesis, we established HLI in C57BL/6 mice (Supplementary Fig. 1). We checked miR-181b expression in the gastrocnemius muscle at different time points after HLI induction by RT-PCR. The expression levels of miR-181b were significantly decreased on day 2 to day 7 after HLI induction (Fig. 1b).

### miR-181b suppressed HUVEC migration and tube formation

To investigate whether miR-181b was involved in angiogenesis, miR-181b was overexpressed or knocked down by transfection with a mimic or inhibitor, and the efficiency of miR-181b overexpression was verified by RT-PCR. The miR-181b mimic resulted in 40-fold overexpression of miR-181b in HUVECs (Supplementary Fig. 2a), and the miR-181b inhibitor reduced miR-181b expression by 70% in HUVECs (Supplementary Fig. 2b). In the Transwell migration assay, miR-181b inhibited the number of HUVECs that migrated through the membrane, whereas the number of migrated cells was increased in the miR-181b inhibitor group compared with the NC group (Fig. 2a, b). To further investigate the role of miR-181b in ECs in vitro, we conducted vascular network formation assays in Matrigel. The miR-181b mimic-inhibited network tube formation, whereas the miR-181b inhibitor significantly increased tube formation (Fig. 2c, d). These results indicated that miR-181b affected endothelial angiogenesis by suppressing migration and tube formation.

### miR-181b inhibited neovascularization in vivo

To investigate whether miR-181b affected angiogenesis in vivo, HLI was surgically induced in C57BL/6 mice that were preinjected with either agomir-NC, agomir-181b,

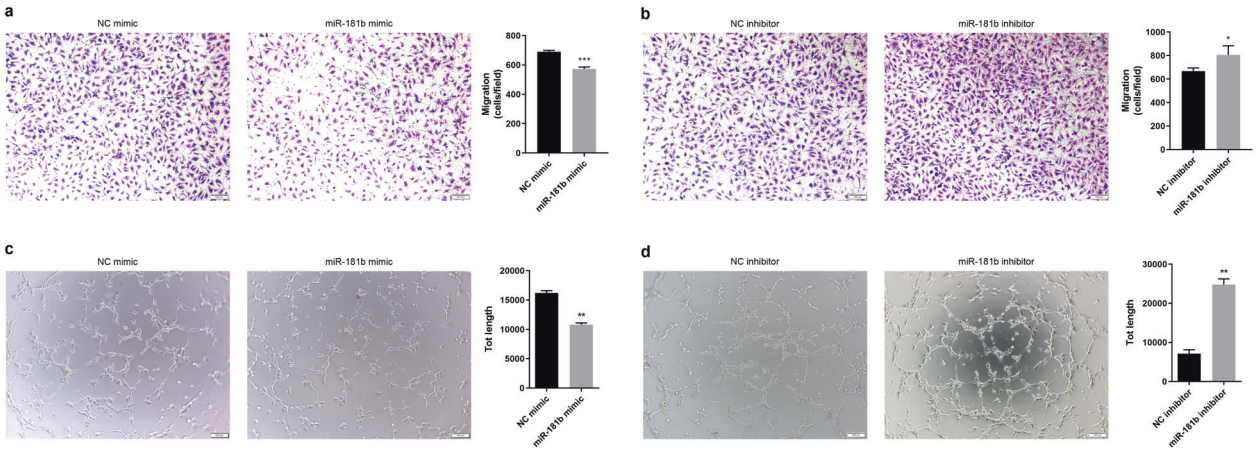


**Fig. 2 miR-181b inhibited endothelial angiogenesis in vitro.** **a** Representative images of EC migration of HUVECs transfected with NC mimic and miR-181b mimic in Transwell chambers. **b** Representative images of EC migration of HUVECs transfected with NC inhibitor and miR-181b inhibitor in Transwell chambers. **c** Representative images of tube-like network formation of HUVECs transfected with NC mimic and miR-181b mimic in Matrigel. **d** Representative images of tube-like network formation of HUVECs transfected with NC inhibitor and miR-181b inhibitor in Matrigel. All the data are represented as the mean ± SEM ($n = 3$), $*P < 0.05$; $**P < 0.01$; $***P < 0.001$ compared with NC mimic or NC inhibitor.

antagomir-NC, or antagomir-181b. Relevant data, such as overexpression and knockdown in vivo and changes in miR-181b expression in HLI, can be seen in Supplementary Fig. 3. Unsurprisingly, 7 days after the operation, the agomir-181b-treated group showed impaired perfusion recovery, and the antagomir-181b-treated group recovered better than the antagomir-NC-treated group (Fig. 3a). These data were further corroborated by a quantitative analysis of capillary density in histological tissue sections from the ischemic gastrocnemius muscle on day 14 after the surgery. As shown in Fig. 3b, immunostaining of IB4-positive cells (endothelial cells) and α-SMA-positive cells (vessel smooth muscle cells) demonstrated a significant increase in the capillary density of the ischemic muscles in the antagomir-181b group and a visible decrease in the capillary density of the ischemic muscles in the agomir-181b group.

To further determine the anti-angiogenic properties of miR-181b, Matrigel plugs were subcutaneously injected into mice and harvested after 7 days. Macroscopically, compared with plugs containing cells pretransfected the scramble control, plugs containing cells pretransfected with antagomir-181b presented as deep red, demonstrating that a large number of new blood vessels had formed in the plugs. The plugs containing agomir-181b presented as light red, implying that there were very few blood vessels in the plugs. HE staining revealed the presence of blood vessels lined with endothelial cells of very different sizes that contained varying amounts of erythrocytes, whereas these cells were barely detected in the agomir-181b group (Fig. 3c).

Altogether, the results demonstrated that miR-181b inhibited capillary outgrowth.

## CCN1 is a direct target of miR-181b

To further explore the molecular mechanism by which miR-181b inhibited HUVEC angiogenic activity, we predicted one putative miR-181b-binding site in the CCN1 3′UTR by TargetScan (Fig. 4a). To confirm whether miR-181b-5p can directly target CCN1, luciferase reporters containing the WT or mutant CCN1 3′-UTR coding sequences were generated. Overexpression of miR-181b significantly repressed the luciferase activity of the WT reporter plasmids but not that of the MUT reporter plasmids (Fig. 4b).

These results provide direct evidence for the miR-181b-mediated regulation of CCN1. Subsequently, we further verified the effect of miR-181b on regulating CCN1 expression at the protein level. Western blot results revealed that compared to their counterparts, miR-181b overexpression sharply decreased the CCN1 protein level, while miR-181b knockdown evidently increased the CCN1 protein level in HUVECs (Fig. 4c, d). These data indicated that miR-181b negatively regulated CCN1 expression in HUVECs.

It has been previously reported that p-AMPK is involved in CCN1-mediated endothelial cell migration and tubular formation. Therefore, to explore whether miR-181b plays a role in this pathway, Western blot analysis was performed to determine the expression of phosphorylated AMPK. The results showed that the overexpression of miR-181b reduced CCN1 and phosphorylated AMPK, whereas inhibition of miR-181b caused apparent increases (Fig. 4c, d). In addition, the expression of CCN1 was miR-181b concentration-dependent (Supplementary Fig. 4a, b). Moreover, hypoxia or limb ischemia can upregulate the mRNA and protein expression of CCN1, and AMPK phosphorylation

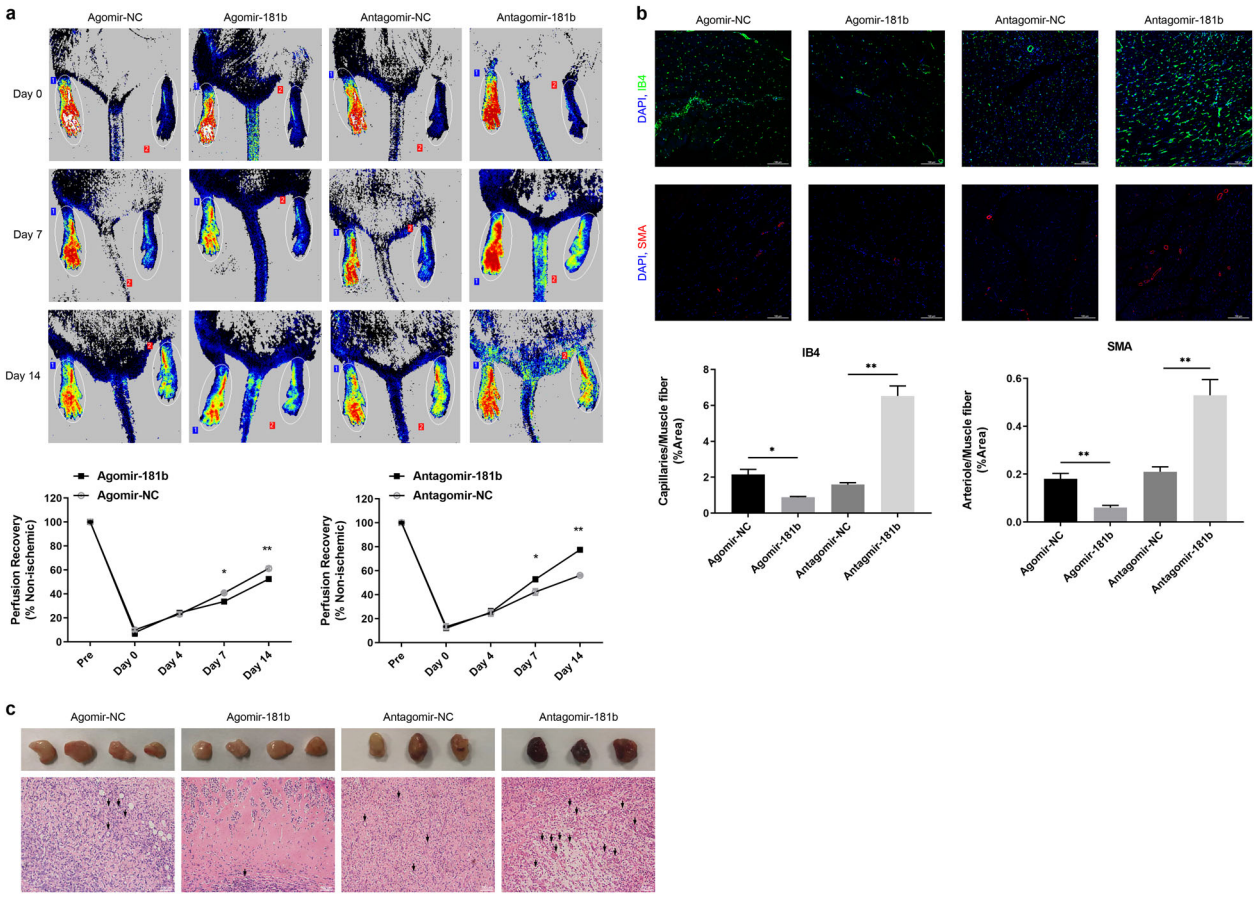


**Fig. 3 miR-181b hindered neovascularization in vivo. a** The hindlimb blood perfusion model injected with agomir-NC, agomir-181b, antagomir-NC, and antagomir-181b was evaluated via laser Doppler imaging on day 0, day 7, and day 14 after HLI. Quantification of the ratio of the injured (HLI) and uninjured (non-HLI) limbs is shown below. $n = 5$ for each group, $^{*}P < 0.05$; $^{**}P < 0.01$ compared with scramble. **b** Fourteen days after HLI, gastrocnemius, and adductor muscles were harvested from the HLI limb, and capillary density was stained with IB4 and α-SMA antibodies. Quantification is shown below. **c** Representative photos and histological images of the effects of miR-181b on Matrigel plug angiogenesis are shown ($n = 4$ in Agomir groups. $n = 3$ in Antagomir groups), the newly formed blood vessels were pointed by arrows.

(Fig. 4e–h). Furthermore, agomir-181b can downregulate the mRNA and protein expression of CCN1, and AMPK phosphorylation in HLI model. And antagomir-181b can upregulate the mRNA and protein expression of CCN1, and AMPK phosphorylation in HLI model (Fig. 4i–l).

## CCN1 restored the miR-181b-regulated phosphorylated AMPK expression and tube-like network formation

We further found that miR-181b-mediated suppression of phosphorylated AMPK could be reversed by overexpression of CCN1 (Fig. 5a). The tubular capacity and migration of endothelial cells, which was inhibited by miR-181b, could be restored by the overexpression of CCN1 (Fig. 5b, c). Moreover, miR-181b inhibitor-mediated increase of phosphorylated AMPK could be reversed by CCN1 sh (Fig. 5d). The tubular capacity and migration of endothelial cells, which was increased by miR-181b inhibitor, could be reversed by CCN1 sh (Fig. 5e, f). In addition, miR-181b inhibitor-mediated increase of phosphorylated AMPK could be reversed by the AMPK inhibitor Compound C [13] (Fig. 5g). The tubular capacity and migration of endothelial cells, which was increased by miR-181b inhibitor, could be reversed by Compound C (Fig. 5h, i).

Altogether, the results demonstrate that miR-181b inhibits the AMPK signaling pathway by reducing the expression of CCN1.

## Expression of miR-181b and CCN1 in human samples

To explore the expression of miR-181b and CCN1 in human samples, amputation specimens were collected. The NC group is patient with amputation in a car accident, and the disease group is a long-term chronic Diabetes patient with diabetic vascular disease. The expression of

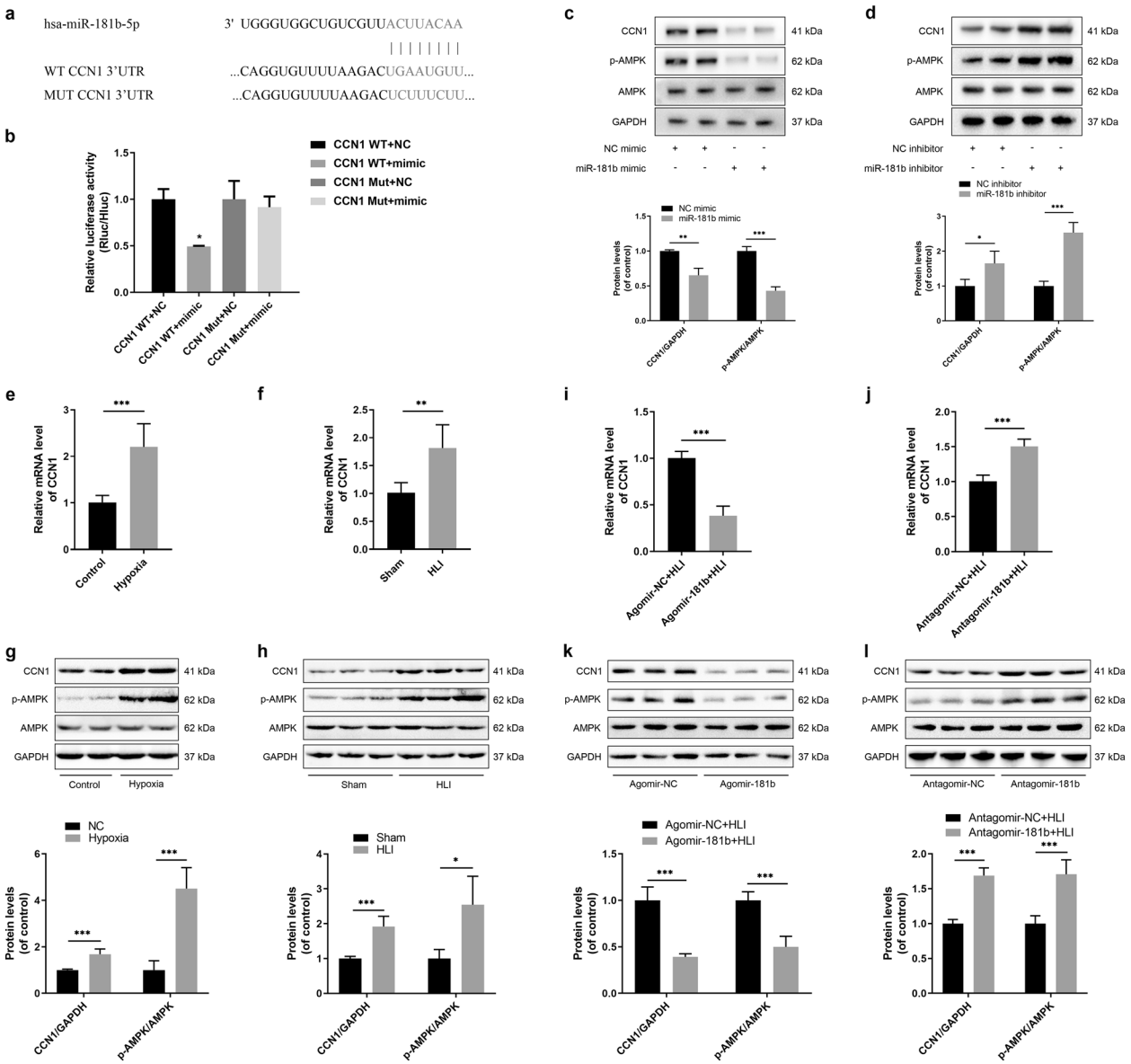


**Fig. 4 miR-181b directly targeted CCN1. a** miR-181b target gene prediction with the bioinformatics tool (TargetScan) is shown. **b** Luciferase activity in 293T cells in the presence of the miR-181b mimic is shown. Data are presented as the mean ± SEM ($n = 3$), $^{*}p < 0.05$ compared with CCN1 WT + NC. **c** Representative Western blot analysis of CCN1 expression and AMPK phosphorylation level in NC mimic and miR-181b mimic group. $^{**}p < 0.01$; $^{***}P < 0.001$ compared with NC mimic. **d** Representative Western blot analysis of CCN1 expression and AMPK phosphorylation level in NC inhibitor and miR-181b inhibitor group. $^{*}p < 0.05$; $^{***}P < 0.001$ compared with NC inhibitor. **e** The mRNA level of CCN1 was detected in HUVECs after exposure to hypoxia for 24 h and Control. $^{***}P < 0.001$ compared with Control. **f** The mRNA level of CCN1 was detected in HLI and Sham limbs. $^{**}P < 0.01$ compared with Sham. **g** Representative western blot analysis of CCN1 expression and AMPK phosphorylation level in HUVECs after exposure to hypoxia for 24 h and Control. $^{***}P < 0.001$ compared with Control. **h** Representative western blot analysis of CCN1 expression and AMPK phosphorylation level in HLI and Sham limbs. $^{*}P < 0.05$; $^{***}P < 0.001$ compared with Sham. **i** The mRNA level of CCN1 was detected in HLI limbs injected with Agomir-NC or Agomir-181b. $^{***}P < 0.001$ compared with Agomir-NC + HLI. **j** The mRNA level of CCN1 was detected in HLI limbs injected with Antagomir-NC or Antagomir-181b. $^{***}P < 0.001$ compared with Antagomir-NC + HLI. **k** Representative Western blot analysis of CCN1 expression and AMPK phosphorylation level in HLI limbs injected with Agomir-NC or Agomir-181b. $^{***}P < 0.001$ compared with Agomir-NC + HLI. **l** Representative western blot analysis of CCN1 expression and AMPK phosphorylation level in HLI limbs injected with Antagomir-NC or Antagomir-181b. $^{***}P < 0.001$ compared with Antagomir-NC + HLI.

miR-181b was significantly higher in limb muscles of Diabetes than NC group (Fig. 6a). The mRNA level of CCN1 was significantly lower in limb muscles of Diabetes than NC group (Fig. 6b). Western blot showed the protein levels of CCN1 and its downstream p-AMPK were lower in limb muscles of Diabetes than NC group (Fig. 6c). And

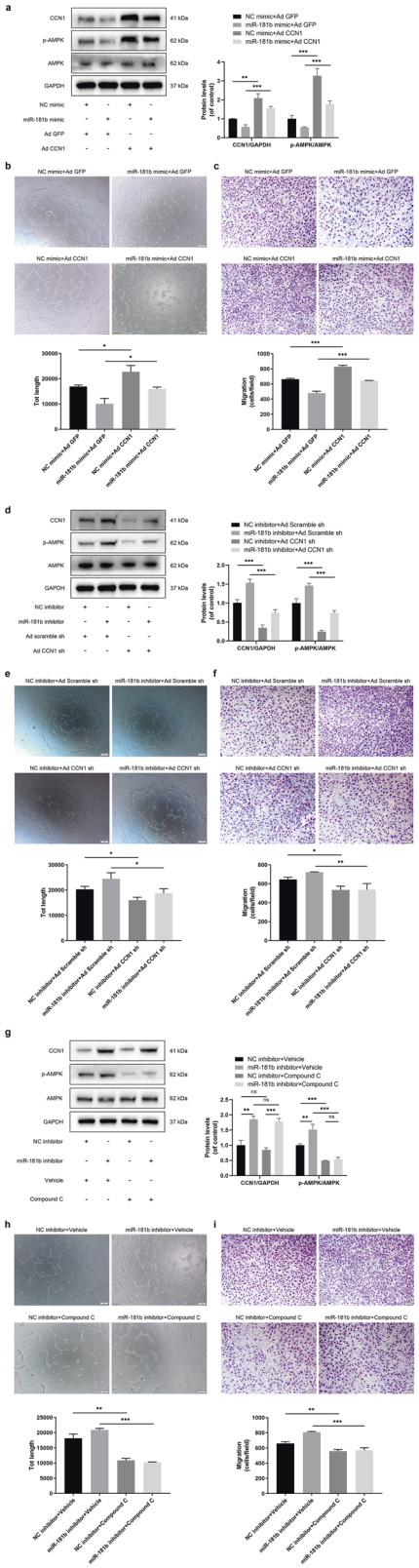

**Fig. 5 CCN1 restored miR-181b-regulated phosphorylated AMPK expression and tube-like network formation. a** CCN1 restored miR-181b-regulated p-AMPK expression. $^{**}p < 0.01$; $^{***}P < 0.001$. **b** CCN1 restored miR-181b mimic-inhibited tube-like network formation. $n = 3$, $^{*}p < 0.05$. **c** CCN1 restored miR-181b mimic-inhibited migration. $n = 3$, $^{***}P < 0.001$. **d** CCN1 shRNA restored miR-181b inhibitor-regulated p-AMPK expression. $^{***}P < 0.001$. **e** CCN1 shRNA restored miR-181b inhibitor-induced tube-like network formation. $n = 3$, $^{*}p < 0.05$. **f** CCN1 shRNA restored miR-181b inhibitor-induced migration. $n = 3$, $^{*}p < 0.05$; $^{**}P < 0.01$. **g** Compound C restored miR-181b inhibitor-regulated p-AMPK expression. $^{**}P < 0.01$; $^{***}P < 0.001$. **h** Compound C restored miR-181b inhibitor-induced tube-like network formation. $n = 3$, $^{**}P < 0.01$; $^{***}P < 0.001$. **i** Compound C restored miR-181b inhibitor-induced migration. $n = 3$, $^{**}P < 0.01$; $^{***}P < 0.001$.

muscle in NC and Diabetes group were co-stained with CCN1 and IB4 (endothelial Marker) by immunofluorescence, it showed that CCN1 has dropped significantly in Diabetes group both in the small to medium blood vessels and the capillaries.

## Discussion

In recent years, miRNAs have been shown to play important roles in embryonic angiogenesis and vascular occlusive diseases. Recently, a series of studies indicated that miR-181b likely plays an essential role in the regulation of angiogenesis. Xu et al. found that miR-181b promotes angiogenesis in retinoblastoma [14], while Cui et al. and Sun et al. found that miR-181b inhibits the migration and tube formation of EA.hg926 and HUVECs in vitro [15, 16]. We demonstrated that miR-181b expression was downregulated in hypoxia-stimulated HUVECs and an HLI model. Our study showed that miR-181b inhibited HUVEC migration and tube formation in vitro and that agomir-181b suppressed perfusion recovery in the HLI model and capillary density in a Matrigel plug assay in vivo. Our results verified that miR-181b had the ability to regulate angiogenesis both in vivo and in vitro.

To explore the molecular mechanism, we predicted one putative miR-181b-binding site in the 3′UTR of CCN1. The CCN family is a new class of extracellular signal regulators. The classic members of this family consist of four conserved modules connected in tandem, each of which is rich in cysteines and highly interactive with other molecules. Members of the mammalian CCN family, particularly CCN1, CCN2, and CCN3, have been described to play multiple roles in mesenchymal development, including the induction and formation of blood vessels [17]. CCN1, also known as CYR61, is not only the first identified member of the CCN family but also the first member described to be an angiogenic factor [18]. CCN1 promotes neovascularization by promoting migration and adhesion, which are mainly mediated by integrins [19, 20]. CCN1 is also thought to play an essential role in organizing endothelial cells to build

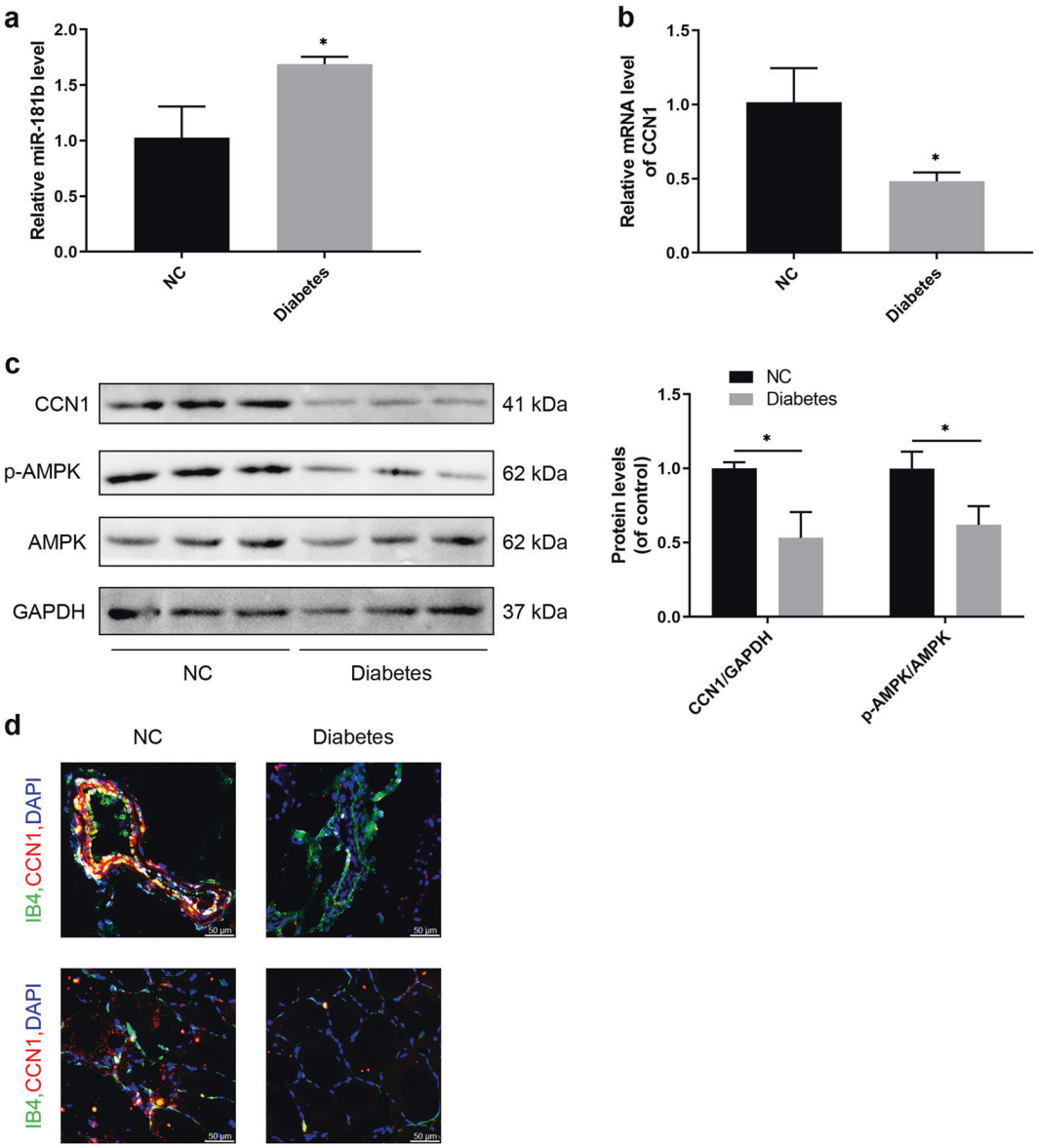


**Fig. 6 The expression of miR-181b and CCN1 in human gastrocnemius muscle. a** The expression of miR-181b was detected in NC and Diabetes. $*p < 0.05$. **b** The mRNA level of CCN1 was detected in NC and Diabetes. $*P < 0.05$. **c** Representative Western blot analysis of CCN1 expression and AMPK phosphorylation level in NC and Diabetes. $n = 3$, $*p < 0.05$. **d** Muscle in NC and Diabetes patient were co-stained with CCN1 and IB4 (endothelial Marker) by immunofluorescence, the upper picture shows the small and medium blood vessels, the lower picture shows the capillaries.

almost all types of vascular structures [21]. We showed with a luciferase reporter assay that miR-181b directly targets CCN1. miR-181b decreased the CCN1 protein levels in HUVECs. These data indicated that miR-181b negatively regulated CCN1 in HUVECs. Therefore, further exploration of the molecular biological mechanism by which CCN1 exerts its pro-angiogenic effect will be helpful for the treatment of ischemic diseases.

Previously, it has been reported that overexpression of CCN1 promotes the migration and survival of cancer cells through AKT or ERK. However, Park et al. [20] found that this result could not be reproduced in HUVECs. In contrast, the AMPK signaling pathway is involved in the CCN1-mediated migration and tube formation of HUVECs. Our results also showed that when miR-181b knockdown caused an increase in CCN1, the downstream level of phosphorylated AMPK also increased. In addition, knocking down CCN1 or applying Compound C, an AMPK inhibitor, can reverse this change, which further validates the viewpoint of Park et al.

In summary, our research indicates that miR-181b is an anti-angiogenic miRNA. In vitro, miR-181b inhibited HUVEC migration and tube formation, and in vivo, inhibition of miR-181b promoted angiogenesis in the HLI and

Matrigel plug assay. The regulation of miR-181b is achieved at least in part by targeting CCN1 to inhibit the AMPK signaling pathway. MiR-181b can be used as a new target for the development of therapies that regulate angiogenesis, and our research will provide new clues for this development.

**Author contributions** ML, JZ, and KH conceived and designed the experiments. YL and SF performed the experiments and prepared the paper. WX and BQ participated in discussions of data analysis. ML, JZ, and KH revised the paper. All the authors gave final approval.

**Funding** This study was funded by the Ministry of Science and Technology of China grant 2016 YFA0101100, the National Natural Science Foundation of China (No: 91949201 and No: 81830014) and Wuhan Science and Technology Plan Project (2018060401011328), and Natural Science Foundation of Hubei Province (2020CFB429).

## Compliance with ethical standards

**Conflict of interest** The author declares no competing interests.

**Publisher's note** Springer Nature remains neutral with regard to jurisdictional claims in published maps and institutional affiliations.

## References

1. Carmeliet P, Jain RK. Molecular mechanisms and clinical applications of angiogenesis. Nature. 2011;473:298–307.
2. Annex BH, Beller GA. Towards the development of novel therapeutics for peripheral artery disease. Trans Am Clin Climatol Assoc. 2016;127:224–34.
3. Folkman J. Angiogenesis in cancer, vascular, rheumatoid and other disease. Nat Med. 1995;1:27–31.
4. Inampudi C, Akintoye E, Ando T, Briasoulis A. Angiogenesis in peripheral arterial disease. Curr Opin Pharmacol. 2018;39:60–7.
5. Icli B, Wara AK, Moslehi J, Sun X, Plovie E, Cahill M, et al. MicroRNA-26a regulates pathological and physiological angiogenesis by targeting BMP/SMAD1 signaling. Circ Res. 2013;113:1231–41.
6. Karamysheva AF. Mechanisms of angiogenesis. Biochemistry. 2008;73:751–62.
7. Carmeliet P. Mechanisms of angiogenesis and arteriogenesis. Nat Med. 2000;6:389–95.
8. Napoleone F. The role of VEGF in the regulation of physiological and pathological angiogenesis. EXS. 2005;94:209–31.
9. Chung AS, Ferrara N. Developmental and pathological angiogenesis. Annu Rev Cell Dev Biol. 2011;27:563–84.
10. Yang WJ, Yang DD, Na S, Sandusky GE, Zhang Q, Zhao G. Dicer is required for embryonic angiogenesis during mouse development. J Biol Chem. 2005;280:9330–5.
11. Bonauer A, Carmona G, Iwasaki M, Mione M, Koyanagi M, Fischer A, et al. MicroRNA-92a controls angiogenesis and functional recovery of ischemic tissues in mice. Science. 2009;324:1710–3.
12. Grundmann S, Hans FP, Kinniry S, Heinke J, Helbing T, Bluhm F, et al. MicroRNA-100 regulates neovascularization by suppression of mammalian target of rapamycin in endothelial and vascular smooth muscle cells. Circulation. 2011;123:999–1009.
13. Zhao Q, Zheng K, Ma C, Li J, Zhuo L, Huang W, et al. PTPS facilitates compartmentalized LTBP1 S-nitrosylation and promotes tumor growth under hypoxia. Mol Cell. 2020;77:95–107. e105.
14. Xu X, Ge S, Jia R, Zhou Y, Song X, Zhang H, et al. Hypoxia-induced miR-181b enhances angiogenesis of retinoblastoma cells by targeting PDCD10 and GATA6. Oncol Rep. 2015;33:2789–96.
15. Cui Y, Han Z, Hu Y, Song G, Hao C, Xia H, et al. MicroRNA-181b and microRNA-9 mediate arsenic-induced angiogenesis via NRP1. J Cell Physiol. 2012;227:772–83.
16. Sun T, Yin L, Kuang H. miR-181a/b-5p regulates human umbilical vein endothelial cell angiogenesis by targeting PDGFRA. Cell Biochem Funct. 2020;38:222–30.
17. Kubota S, Takigawa M. CCN family proteins and angiogenesis: from embryo to adulthood. Angiogenesis. 2007;10:1–11.
18. Babic AM, Kireeva ML, Kolesnikova TV, Lau LF. CYR61, a product of a growth factor-inducible immediate early gene, promotes angiogenesis and tumor growth. Proc Natl Acad Sci USA. 1998;95:6355–60.
19. Menendez JA, Vellon L, Mehmi I, Teng PK, Griggs DW, Lupu R. A novel CYR61-triggered 'CYR61-alphavbeta3 integrin loop' regulates breast cancer cell survival and chemosensitivity through activation of ERK1/ERK2 MAPK signaling pathway. Oncogene. 2005;24:761–79.
20. Park YS, Hwang S, Jin YM, Yu Y, Jung SA, Jung SC, et al. CCN1 secreted by tonsil-derived mesenchymal stem cells promotes endothelial cell angiogenesis via integrin αv β3 and AMPK. J Cell Physiol. 2015;230:140–9.
21. Goodwin CR, Lal B, Zhou X, Ho S, Xia S, Taeger A, et al. Cyr61 mediates hepatocyte growth factor-dependent tumor cell growth, migration, and Akt activation. Cancer Res. 2010;70:2932–41.